












# Diagnostic Accuracy of Screening Arterial Spin-Labeling MRI Using Hadamard Encoding for the Detection of Reduced CBF in Adult Patients with Ischemic Moyamoya Disease

 K. Setta,  T. Matsuda,  M. Sasaki,  T. Chiba,  S. Fujiwara,  M. Kobayashi,  K. Yoshida,  Y. Kubo,  M. Suzuki,  K. Yoshioka, and  K. Ogasawara



## ABSTRACT

**BACKGROUND AND PURPOSE:** Adult patients with ischemic Moyamoya disease are advised to undergo selective revascularization surgery based on cerebral hemodynamics. The purpose of this study was to determine the diagnostic accuracy of arterial spin-labeling MR imaging using Hadamard-encoded multiple postlabeling delays for the detection of reduced CBF in such patients.

**MATERIALS AND METHODS:** Thirty-seven patients underwent brain perfusion SPECT and pseudocontinuous arterial spin-labeling MR imaging using standard postlabeling delay (1525 ms) and Hadamard-encoded multiple postlabeling delays. For Hadamard-encoded multiple postlabeling delays, based on data obtained from the 7 sub-boluses with combinations of different labeling durations and postlabeling delays, CBF corrected by the arterial transit time was calculated on a voxel-by-voxel basis. Using a 3D stereotaxic template, we automatically placed ROIs in the ipsilateral cerebellar hemisphere and 5 MCA territories in the symptomatic cerebral hemisphere; then, the ratio of the MCA to cerebellar ROI was calculated.

**RESULTS:** The area under the receiver operating characteristic curve for detecting reduced SPECT-CBF ratios ( $<0.686$ ) was significantly greater for the Hadamard-encoded multiple postlabeling delays–CBF ratios (0.885) than for the standard postlabeling delay–CBF ratios (0.786) ( $P = .001$ ). The sensitivity and negative predictive value for the Hadamard-encoded multiple postlabeling delays–CBF ratios were 100% (95% confidence interval, 100%–100%) and significantly higher than the sensitivity (95% CI, 44%–80%) and negative predictive value (95% CI, 88%–97%) for the standard postlabeling delay–CBF ratio, respectively.

**CONCLUSIONS:** ASL MR imaging using Hadamard-encoded multiple postlabeling delays may be applicable as a screening tool because it can detect reduced CBF on brain perfusion SPECT with 100% sensitivity and a 100% negative predictive value in adult patients with ischemic Moyamoya disease.

**ABBREVIATIONS:** ASL = arterial spin-labeling; ATT = arterial transit time; hASL = Hadamard-encoded multiple PLD ASL; MMD = Moyamoya disease; PLD = postlabeling delay; sASL = standard-encoded PLD ASL

Moyamoya disease (MMD) is a chronic, occlusive cerebrovascular disease of unknown etiology that is characterized by bilateral steno-occlusive changes in the terminal portion of the ICA and an abnormal vascular network at the base of the brain.<sup>1,2</sup> The typical treatment for patients with ischemia symptoms is


revascularization surgery, which can involve anastomosis of the superficial temporal artery and MCA.<sup>3</sup> Regardless of the severity of cerebral ischemia, this procedure is universally recommended for pediatric patients with MMD with ischemic symptoms because in such cases, the brain is still developing.<sup>3–5</sup> By contrast, revascularization surgery is selectively recommended for adult patients presenting with ischemic symptoms.<sup>3,6</sup> However, no clear guidelines are available for this selection. Two recent studies used PET and brain perfusion SPECT to measure the oxygen extraction fraction and CBF, respectively, and demonstrated that among adult patients (older than 30 but younger than 60 years of age) receiving medication alone for symptomatic ischemic MMD without hemodynamic compromise, such as misery perfusion or reduced CBF, the incidence of recurrent ischemic events was very low (approximately 1% per year).<sup>7,8</sup> Moreover, the recurrent ischemic episodes were transient ischemic attacks only, and no changes were seen in scores on the modified Rankin Disability

Received December 28, 2020; accepted after revision March 11, 2021.

From the Department of Neurosurgery (K.S., T.C., S.F., M.K., K. Yoshida, Y. Kubo, K.O.), Department of Radiology (M. Suzuki, K. Yoshioka), and Division of Ultrahigh Field MRI, Institute for Biomedical Sciences (T.M., M. Sasaki), Iwate Medical University School of Medicine, Yahaba-cho, Japan.

This study was funded by a Grant-in-Aid for Scientific Research from the Japan Society for the Promotion of Science (JP18K09002).

Please address correspondence to Kuniaki Ogasawara, MD, Department of Neurosurgery, Iwate Medical University, Idaidoori 2-1-1, Yahaba-cho 020-8505, Japan; e-mail: kuogasa@iwate-med.ac.jp

 Indicates open access to non-subscribers at [www.ajnr.org](http://www.ajnr.org)

 Indicates article with online supplemental data.

<http://dx.doi.org/10.3174/ajnr.A7167>

Scale after the recurrence of ischemic symptoms in such patients.<sup>7</sup> In addition, neither cerebral hemodynamics nor cognitive function had deteriorated at 2 years after the last event in patients without recurrent ischemic events.<sup>7</sup> Initial treatment with medication alone may be recommended for adult patients with ischemic MMD without hemodynamic compromise,<sup>7</sup> and the determination of whether hemodynamic compromise exists in the symptomatic cerebral hemisphere is important for the management of such patients.<sup>7,8</sup> However, the clinical use of PET or brain perfusion SPECT to detect misery perfusion or reduced CBF is precluded by its high cost and limited availability in the clinical setting. Other screening modalities for detecting hemodynamic compromise before performing PET or brain perfusion SPECT would therefore be useful.

Arterial spin-labeling (ASL) MR imaging is a noninvasive technique that can quantify CBF.<sup>9-11</sup> A number of studies involving patients with MMD conducted using ASL MR imaging with a single postlabeling delay (PLD) have simply compared CBF measured using ASL MR imaging with brain perfusion parameters measured using other modalities such as PET, SPECT, and dynamic susceptibility contrast perfusion MR imaging.<sup>12-14</sup> However, almost all the cerebral cortical regions in MMD have some degree of perfusion delay, which varies even within individual cerebral cortical regions of a single patient.<sup>15</sup> Therefore, it is difficult to obtain precise CBF measurements using the standard ASL method with a single PLD in MMD.<sup>15</sup> By contrast, theoretically, ASL measurements covering a wide range of PLD times can be interpreted to estimate CBF with practical spatial and temporal resolutions in the clinical setting.<sup>16,17</sup> Actually, multi-PLD ASL MR imaging with corrections using the arterial transit time (ATT) significantly improved CBF quantification compared with single-PLD ASL MR imaging.<sup>18,19</sup> However, the accuracy of multi-PLD ASL MR imaging for detecting hemodynamic compromise has not been reported. Hadamard-encoding techniques have recently been applied to the ASL methods to calculate the ASL signals as multiple PLDs by dividing the ASL signal into sub-boluses of different PLDs.<sup>16</sup> Several investigations have demonstrated that Hadamard-encoded labeling strategies for healthy human subjects provide robust CBF measurements in a time-efficient manner with shorter scan times (<10 minutes).<sup>20</sup> This benefit may be suitable for the detection of reduced CBF in patients with MMD.

Given this background, the aims of this study were to determine the diagnostic accuracy of ASL MR imaging using Hadamard-encoded multiple PLDs for the detection of reduced CBF, a key determinant for revascularization surgery, in adult patients with ischemic MMD, and to propose practical clinical algorithms using ASL MR imaging and subsequent management in such patients.

## MATERIALS AND METHODS

The protocol of the present prospective observational study was reviewed and approved by our institutional ethics committee. Written, informed consent was obtained from all participants or their next of kin before the study began.

### Patients

Patients who were diagnosed as having MMD according to the diagnostic criteria of the Research Committee on Spontaneous

Occlusion of the Circle of Willis of the Ministry of Health, Labor, and Welfare of Japan<sup>1</sup> were prospectively selected for participation in this study if they satisfied the following clinical inclusion criteria: older than 30 but younger than 60 years of age, modified Rankin disability scale score of 0 or 1, presence of episodes of ischemic symptoms in the unilateral carotid territory occurring  $\leq 3$  months before presentation to our department, and absence of infarction in the bilateral cerebral cortices on MR imaging.

### Brain Perfusion SPECT

A brain perfusion SPECT study was performed using *N*-isopropyl-p-[<sup>123</sup>I]iodoamphetamine (<sup>123</sup>I-IMP) and a triple-head gamma camera (GCA-9300R; Toshiba Medical Systems) between 3 weeks and 3 months after the last ischemic event. The spatial resolution of the gamma camera with a high-resolution fan-beam collimator was 8.5-mm full width at half maximum. The SPECT acquisition protocol consisted of a matrix size of 128  $\times$  128 and a 30-minute continuous acquisition (5 minutes/rotation) over 360° in 4° steps. Postacquisition, the data were corrected for scatter using the triple energy window method and then reconstructed by filtered back-projection. A Butterworth preprocessing filter was applied with a cutoff frequency of 0.08 cycles per pixel (1 pixel = 1.72 mm). For attenuation correction, the iterative Chang method was used,<sup>21</sup> and the attenuation map was generated by extracting the skin contour and assuming the inner region side as a uniform attenuation body. The attenuation coefficient was 0.146 cm<sup>-1</sup>.

After delivering a 1-minute intravenous infusions of 222 MBq of <sup>123</sup>I-IMP (5-mL volume) and physiologic saline at a constant rate of 5 mL/min, data were acquired at a midscan time of 30 minutes after the administration of <sup>123</sup>I-IMP with a scan duration of 20 minutes.<sup>22</sup>

### ASL MRI

ASL MR imaging studies were performed using a 3T MR imaging scanner (Discovery MR750; GE Healthcare) with an 8-channel receive head coil and body coil for transmission within 3 days after the brain perfusion SPECT study. Each patient underwent 2 kinds of ASL MR imaging with a 3D pseudocontinuous labeling sequence. At first, the standard ASL (sASL) was performed using the following parameters: labeling duration, 1450 ms; PLD, 1525 ms; TR, 4802 ms; TE, 10.5 ms; section thickness, 4.0 mm; number of slices, 32; sampling points, 8 arms  $\times$  512; FOV, 24  $\times$  24 cm; matrix size, 128  $\times$  128; and voxel resolution, 1.9  $\times$  1.9  $\times$  4.0 mm. The total scan time was 3 minutes 13 seconds. Next, for ASL MR imaging using Hadamard-encoded multiple PLDs (hASL), we performed ASL consisting of 7 sub-boluses<sup>17</sup> with the following combinations of labeling duration and PLDs: labeling duration (ms), PLD (ms) = 286, 700; 330, 998; 370, 1327; 432, 1697; 534, 2128; 732, 2661; and 1308, 3392, with TR, 6141 ms; TE, 24.3 ms; section thickness, 4.0 mm; number of slices, 32; sampling points, 4 arms  $\times$  512; FOV, 24  $\times$  24 cm; matrix size, 128  $\times$  128; and voxel resolution, 1.9  $\times$  1.9  $\times$  4.0 mm. The total scan time was 7 minutes 35 seconds. For each scan, vessel suppression using a velocity-selective saturation sequence was applied to reduce artifactual bright signals by dephasing intravascular labeled spins.<sup>20</sup> On the basis of data obtained from the 7 sub-boluses, CBF

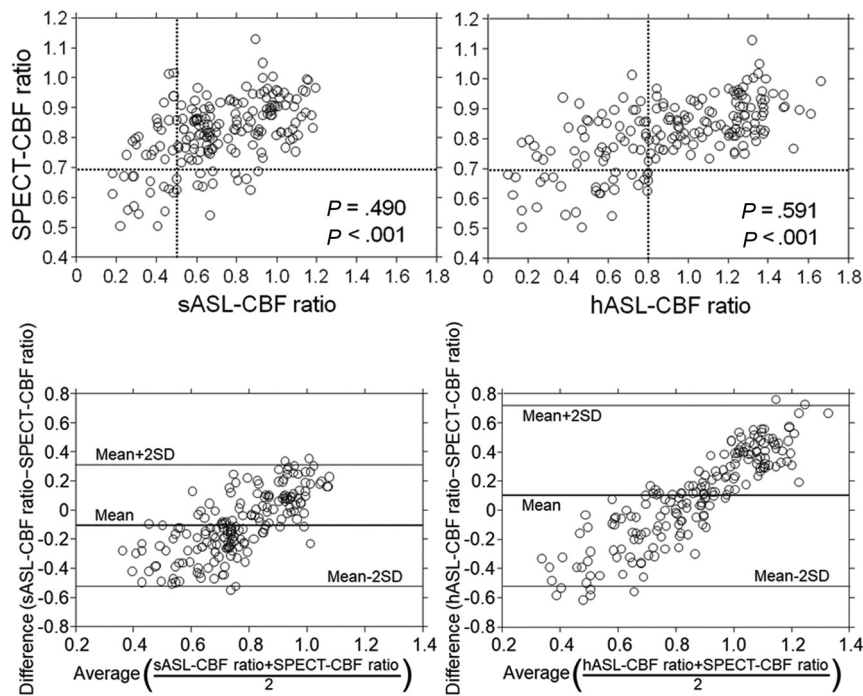


**FIG 1.** Comparisons (upper graphs) and Bland-Altman plots (lower graphs) of SPECT-CBF and sASL-CBF ratios and sASL-CBF (left graphs) or hASL-CBF ratios (right graphs) for each MCA ROI in each patient. In the upper graphs, each horizontal line denotes the cutoff point for indicating a reduced SPECT-CBF ratio (0.686) and each vertical line denotes the cutoff point lying closest to the upper left corner of the receiver operating characteristic curve for detecting a reduced SPECT-CBF ratio (0.502 for sASL-CBF, 0.801 for hASL-CBF).

corrected by the ATT was automatically calculated on a voxel-by-voxel basis.

#### Data Analysis and Definition of Reduced CBF

All SPECT and ASL MR imaging data were transformed into the standard brain size and shape by linear and nonlinear transformation using statistical parametric mapping (SPM2; <http://www.fil.ion.ucl.ac.uk/spm/software/spm12>) for anatomic standardization.<sup>23</sup> Therefore, the brain images from all participants had the same anatomic format. A total of 318 constant ROIs were automatically placed in both the cerebral and cerebellar hemispheres using a 3D stereotaxic ROI template with SPM2.<sup>24</sup> ROIs were grouped into 10 segments—callosomarginal, pericallosal, precentral, central, parietal, angular, temporal, posterior, hippocampal, and cerebellar—in each hemisphere according to the arterial supply. Of these 10 segments, 5—precentral, central, parietal, angular, and temporal—perfused by the MCA and cerebellar ROI were selected for analyses.<sup>22</sup>

The mean values of the radioactive counts on brain perfusion SPECT images and CBF and ATT on ASL MR images were measured in the 5 MCA ROIs in both cerebral hemispheres and both cerebellar ROIs. For each patient, the mean value in each MCA ROI in the symptomatic cerebral hemisphere relative to that in the ipsilateral cerebellar ROI on brain perfusion SPECT and ASL MR imaging was calculated and defined as the SPECT-CBF, ASL-CBF, and ASL-ATT ratios, respectively.

For each MCA ROI of each patient, the ROI was defined as exhibiting reduced CBF when the SPECT-CBF ratio was  $< 0.686$ .<sup>22</sup>

#### Statistical Analysis

Data are expressed as the mean (SD). Correlations between 2 variables were determined using the Spearman rank correlation coefficient. Differences between 2 correlation coefficients were compared using the Meng-Rosenthal-Rubin method. Bland-Altman analysis was performed to confirm the concordance between each CBF ratio. Taking the correlation between different measures in the same patient into account, we evaluated the relationship between SPECT-CBF and ASL-CBF ratios using generalized linear mixed effects models with a subject random intercept. These 2 parameters were assumed to be a normal variable with an identity link. Receiver operating characteristic curves were used to assess the accuracy of the sASL-CBF and hASL-CBF ratios for detecting reduced CBF. Reduced CBF as a criterion standard was defined as a SPECT-CBF ratio of  $< 0.686$ .<sup>22</sup>

Pair-wise comparisons of the area under the receiver operating characteristic curves for the sASL-CBF and hASL-CBF ratios were then performed. For all statistical analyses, significance was set at  $P < .05$ . The exact 95% CIs for sensitivity, specificity, and positive and negative predictive values were computed with binomial distributions. Differences in the sensitivity, specificity, and positive and negative predictive values among the sASL-CBF and hASL-CBF ratios were analyzed using 95% CIs.

#### RESULTS

During the 24-month study period, a total of 40 patients met the inclusion criteria, among whom, 3 declined to participate. The remaining 37 patients (13 men, 24 women; mean age, 45 [SD, 6] years; age range, 31–57 years) underwent brain perfusion SPECT and ASL MR imaging, leading to 185 ( $5 \times 37$ ) MCA ROIs in the symptomatic cerebral hemispheres being included in the final analyses. Among these 37 patients, 29 experienced the onset of transient ischemic attacks alone; 3, a minor stroke alone; and 5, onset of a minor stroke after a transient ischemic attack. In total, 11, 16, and 10 patients were classified into MRA stages 2, 3, and 4, respectively.<sup>1</sup>

A significant positive correlation was observed between SPECT-CBF and sASL-CBF ( $\rho = 0.490$ ;  $P < .001$ ) or hASL-CBF ratios ( $\rho = 0.591$ ;  $P < .001$ ) in the 185 MCA ROIs (Fig 1). The latter coefficient was significantly greater than the former ( $P = .002$ ). A significant positive correlation was also observed between SPECT-CBF ratios and the quantitative values of

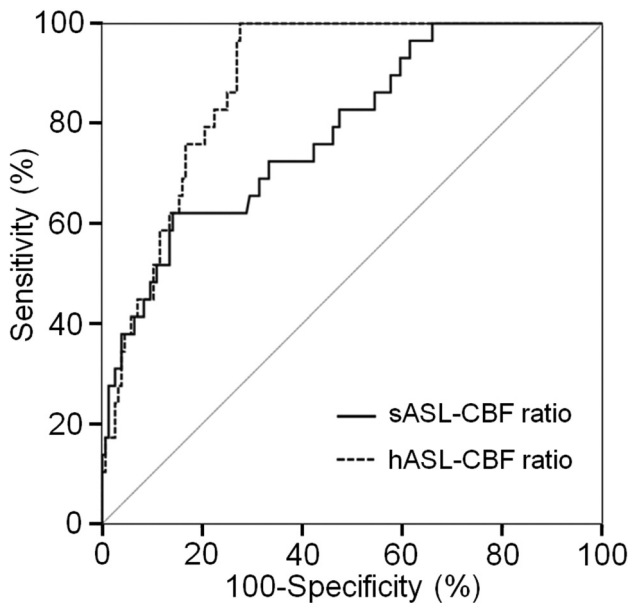


**FIG 2.** Receiver operating characteristic curves used to compare the accuracy of sASL-CBF and hASL-CBF ratios for detecting a reduced SPECT-CBF ratio. Pair-wise comparison analysis shows a significantly greater area under the receiver operating characteristic curve for the hASL-CBF (dotted line) than for the sASL-CBF ratio (solid line).

sASL-CBF ( $\rho = 0.462$ ;  $P < .001$ ) or hASL-CBF ( $\rho = 0.534$ ;  $P < .001$ ) in the 185 MCA ROIs (Online Supplemental Data). Although the former coefficient did not differ from that between SPECT-CBF and sASL-CBF ratios, the latter coefficient was significantly lower than that between SPECT-CBF and hASL-CBF ratios ( $P = .036$ ).

No constant bias was detected for the SPECT-CBF and sASL-CBF (95% CI of difference,  $-0.530$ – $0.319$ ) or hASL-CBF ratios (95% CI of difference,  $-0.510$ – $0.711$ ) by Bland-Altman analysis (Fig 1). However, a proportional bias was identified for SPECT-CBF and sASL-CBF (slope-of-regression equation,  $0.969$ ;  $P < .001$ ) or hASL-CBF ratios (slope-of-regression equation,  $1.242$ ;  $P < .001$ ) (Fig 1). Whereas sASL-CBF ratios showed a propensity toward underestimation at lower CBF ratios, hASL-CBF ratios showed a propensity toward underestimation and overestimation at lower and higher CBF ratios, respectively. Generalized linear mixed effects models with a subject random intercept revealed a significant relationship between SPECT-CBF and sASL-CBF ( $P < .001$ ) or hASL-CBF ratios ( $P < .001$ ).

Of the 185 ROIs analyzed, 29 (16%) were determined to exhibit reduced CBF on brain perfusion SPECT. The areas under the curve for sASL-CBF and hASL-CBF ratios for detecting reduced CBF on brain perfusion SPECT were  $0.786$  (95% CI,  $0.720$ – $0.843$ ) and  $0.885$  (95% CI,  $0.830$ – $0.927$ ), respectively; the latter was significantly greater than the former (difference between areas,  $0.099$ ;  $P = .001$ ) (Fig 2).

The sensitivity and negative predictive value for the hASL-CBF ratio, with the cutoff point lying closest to the upper left corner of the receiver operating characteristic curve for the detection of MCA ROIs with reduced CBF on brain perfusion SPECT, were 100% (cutoff point,  $0.801$ ) and significantly higher than those for the sASL-CBF ratio (cutoff point,  $0.502$ ) (Online

Supplemental Data). The specificity and positive predictive value did not differ between the 2 ASL-CBF ratios.

When the difference between the hASL-CBF and SPECT-CBF ratios (hASL-CBF ratio–SPECT-CBF ratio) was compared with the hASL-ATT ratio for each MCA ROI (Online Supplemental Data), the differences in most MCA ROIs exhibiting nonreduced hASL-CBF ratios ( $\geq 0.801$ ) and nonreduced SPECT-CBF ratios ( $\geq 0.686$ ) were  $>0$ , regardless of the hASL-ATT ratios. By contrast, the differences for most MCA ROIs with reduced hASL-CBF ratios ( $< 0.801$ ) were  $<0$  regardless of the ASL-ATT ratios. In particular, no MCA ROIs with reduced hASL-CBF ratios exhibited reduced SPECT-CBF ratios when they had an hASL-ATT ratio of  $>1.3$ .

Of the 37 patients studied, 1, 3, 6, and 4 patients had 4, 3, 2, and 1 MCA ROIs with reduced CBF on brain perfusion SPECT, respectively. Therefore, 14 patients (38%) were determined to have MCA ROIs with reduced CBF. In the 10 patients with  $\geq 2$  MCA ROIs with reduced CBF, the ROIs were adjacent to one another. The sensitivity and negative predictive value for the hASL-CBF ratio for the detection of patients with MCA ROIs exhibiting reduced CBF on brain perfusion SPECT based on the determination for each MCA ROI were 100% and significantly higher than those for the sASL-CBF ratio (Online Supplemental Data). The specificity and positive predictive value did not differ between these 2 ASL-CBF ratios.

Figures 3 and 4 show representative MRA, brain perfusion SPECT, and ASL MR images in a patient with MCA ROIs exhibiting reduced CBF and in a patient without any MCA ROIs exhibiting reduced CBF, respectively.

## DISCUSSION

The results of this study demonstrate that ASL MR imaging using Hadamard-encoded multiple PLDs can detect reduced CBF on brain perfusion SPECT with 100% sensitivity and negative predictive value in adult patients with ischemic MMD. This diagnostic accuracy may be applicable as a screening test before further examination of cerebral hemodynamics.

In this study, CBF in each MCA ROI in the symptomatic cerebral hemisphere was normalized using CBF in the ipsilateral cerebellar hemisphere. This cerebellar normalization has been commonly applied to brain perfusion SPECT because of its simplicity, objectivity, and reproducibility.<sup>22,25,26</sup> By contrast, the accuracy of the cerebellar normalization for ASL-CBF in patients with MMD remains controversial. One previous study demonstrated improvement of the correlation between sASL-CBF and PET-CBF by cerebellar normalization,<sup>15</sup> whereas another found overestimation of sASL-CBF by cerebellar normalization.<sup>12</sup> Perfusion delay may differ between the cerebral and cerebellar cortexes in healthy subjects, and this difference in perfusion delay may vary in patients with MMD. Our data showed a better correlation between SPECT-CBF ratios and hASL-CBF ratios compared with that between SPECT-CBF ratios and sASL-CBF ratios or between SPECT-CBF ratios and quantitative hASL-CBF values. These findings suggest that correcting brain perfusion delay, including the cerebellum using Hadamard-encoded multiple PLDs, may increase the accuracy of cerebellar normalization for ASL-CBF in MMD. However, this correction also underestimated and overestimated ASL-CBF

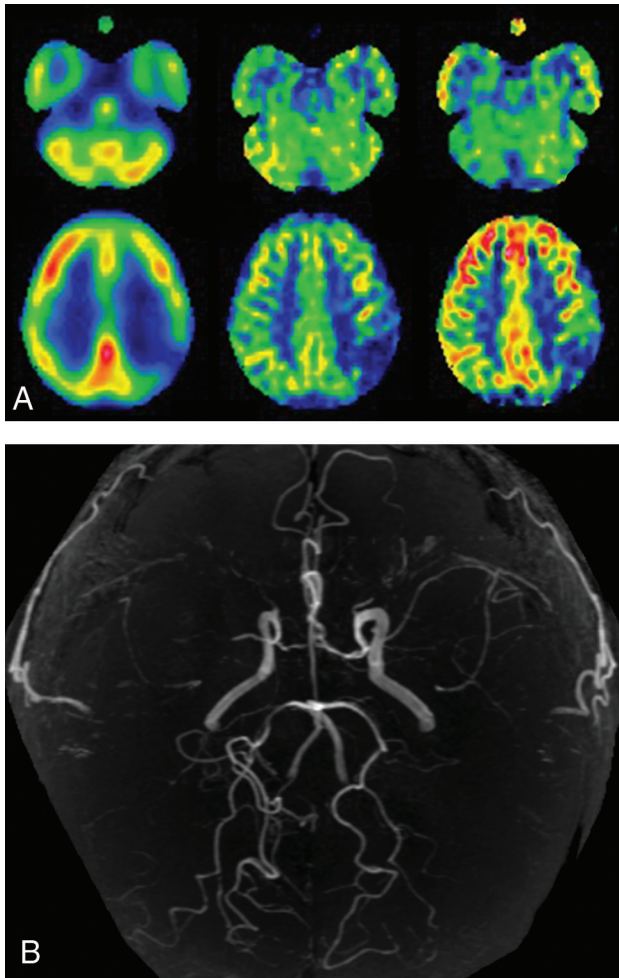


**FIG 3.** MRA (B), brain perfusion SPECT images (A, left), and sASL (A, middle) and hASL (A, right) MR images of a 43-year-old male patient with transient ischemic attacks complicated by right-sided hemiparesis. MRA shows stage 3 Moyamoya disease. On all 3 SPECT and ASL images, the CBF in the left parietal region is severely reduced compared with that in the left cerebellar hemisphere.

ratios at lower and higher CBFs, respectively. We used the vessel-suppression technique for hASL MR imaging to reduce artifactual bright signals by dephasing intravascular labeled spins.<sup>27</sup> However, this technique theoretically prolongs the effective TE, resulting in a reduction in the SNR.<sup>27</sup> Such SNR reductions may be related to the underestimation of hASL-CBF ratios at lower CBFs. Actually, investigators do not necessarily recommend the use of vessel suppression for clinical applications.<sup>27</sup> By contrast, the overestimation of hASL-CBF ratios at higher CBFs may be due to the overcorrection of cerebral perfusion delay using Hadamard-encoded multiple PLDs in cerebral regions with slightly or not prolonged PLDs; these should be considered limitations of hASL MR imaging.

A previous study using PET demonstrated that among adult patients receiving medication alone for symptomatic ischemic MMD without an increased oxygen extraction fraction in all MCA ROIs, the incidence of recurrent ischemic events was very low.<sup>7</sup> Another study showed that SPECT-CBF ratios obtained in the same fashion as in the present study detect increased oxygen

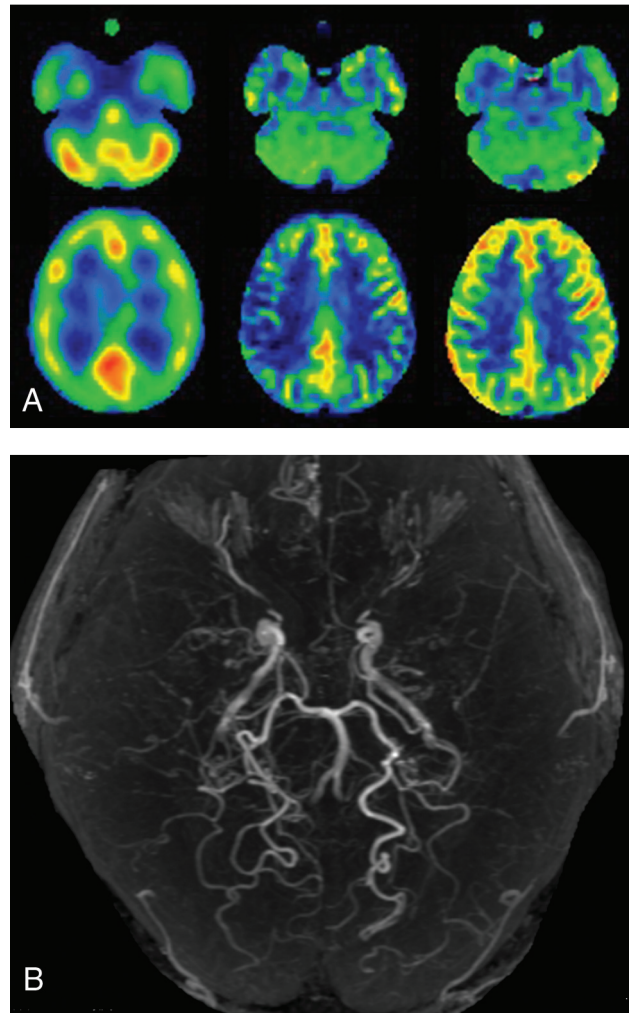


**FIG 4.** MRA (B), brain perfusion SPECT images (A, left), and sALS (A, middle) and hASL (A, right) MR images of a 34-year-old female patient with transient ischemic attacks complicated by left-sided hemiparesis. MRA shows stage 3 Moyamoya disease. On perfusion SPECT images, the CBF in the right MCA territory is slightly reduced compared with that in the right cerebellar hemisphere. The CBF on sALS MR images is severely reduced in the right central, parietal, and angular regions, whereas the CBF on hASL MR imaging is not reduced relative to the right cerebellar hemisphere.

extraction fraction with 100% sensitivity and a 100% negative predictive value in adult patients with ischemic MMD (older than 30 but younger than 60 years of age), and the optimal cutoff point for the SPECT-CBF ratio for detection of increased oxygen extraction fraction is 0.686.<sup>22</sup> The present study, therefore, defined a SPECT-CBF ratio below this cutoff point as reduced CBF. As a result, the sensitivity and negative predictive value of hASL for the detection of reduced CBF on brain perfusion SPECT were 100%. This diagnostic accuracy may be applicable to a screening test before further examination of cerebral hemodynamics. By contrast, the positive predictive value of hASL was low (<50%) and comparable with that of sASL. In particular, reduced CBF on hASL was not corrected when the hASL-ATT ratio was >1.3. This finding suggests that hASL does not

sufficiently correct the longer perfusion delays in the cerebral cortex in patients with MMD, also a limitation of hASL MR imaging.

On the basis of the present data and previous findings,<sup>7,22</sup> we propose practical clinical algorithms for the detection of hemodynamic compromise using ASL MR imaging with Hadamard-encoded multiple PLDs and subsequent management in adult patients with ischemic MMD. Patients who undergo ASL MR imaging using Hadamard-encoded multiple PLDs are determined to not have hemodynamic compromise and should, therefore, receive medication alone, including an antiplatelet drug, if the ASL-CBF ratios in all MCA ROIs in the symptomatic hemisphere are not low ( $\geq 0.801$ ). If the ASL-CBF ratio in any MCA ROI is low ( $< 0.801$ ), the patient may possibly have hemodynamic compromise and, therefore, requires further examinations such as brain perfusion SPECT and/or ( $^{15}\text{O}$ ) gas PET to detect hemodynamic compromise more accurately. If hemodynamic compromise is detected on SPECT or PET, revascularization surgery may be recommended. The introduction of ASL MR imaging using Hadamard-encoded multiple PLDs for screening may reduce the number of patients who undergo PET or brain perfusion SPECT by about two-thirds.

A prospective study<sup>7</sup> reported that during the recurrence of ischemic events in adult patients with MMD, the affected cerebral hemisphere exhibited new misery perfusion. By contrast, cerebral hemodynamics had not deteriorated 2 years after the last event in patients without recurrent ischemic events. Those results suggest that the development of misery perfusion may be a strong predictor of recurrent ischemic events in adult patients with ischemic-onset MMD.<sup>7</sup> The detection of reduced CBF using screening ASL MR imaging with Hadamard-encoded multiple PLDs for such patients may be also recommended for the prediction of recurrent ischemic symptoms during follow-up.

In addition to the limitations listed above, we did not assess stress perfusion such as acetazolamide challenge. A previous study demonstrated that whereas CBF assessed using brain perfusion SPECT detects misery perfusion with high sensitivity and a high negative predictive value in adult patients with ischemic MMD, the accuracy of cerebrovascular reactivity to acetazolamide is significantly lower than that of CBF.<sup>22</sup> Furthermore, cerebrovascular reactivity to acetazolamide in addition to CBF did not increase the accuracy for detecting misery perfusion.<sup>22</sup> These findings suggest that hemodynamic compromise can be sufficiently detected by CBF measurement alone in such patients.<sup>22</sup>

## CONCLUSIONS

ASL MR imaging using Hadamard-encoded multiple PLDs can detect reduced CBF on brain perfusion SPECT with 100% sensitivity and 100% negative predictive value in adult patients with ischemic MMD; therefore, it may be applicable as a screening tool before further examination of cerebral hemodynamics.

Disclosures: Makoto Sasaki—UNRELATED: Grants/Grants Pending: Japan Society for the Promotion of Science-Kakenhi, Hitachi, GE Healthcare\*; Payment for Lectures Including Service on Speakers Bureaus: Hitachi, GE Healthcare. \*Money paid to the institution.

## REFERENCES

1. Research Committee on the Pathology and Treatment of Spontaneous Occlusion of the Circle of Willis; Health Labour Sciences Research Grant for Research on Measures for Intractable Diseases. **Guidelines for diagnosis and treatment of moyamoya disease (spontaneous occlusion of the circle of Willis).** *Neurol Med Chir (Tokyo)* 2012;52:245–66 [CrossRef Medline](#)
2. Suzuki J, Takaku A. **Cerebrovascular “moyamoya” disease: disease showing abnormal net-like vessels in base of brain.** *Arch Neurol* 1969;20:288–99 [CrossRef Medline](#)
3. Fujimura M, Tominaga T. **Current status of revascularization surgery for moyamoya disease: special consideration for its ‘internal carotid-external carotid (IC-EC) conversion’ as the physiological reorganization system.** *Tohoku J Exp Med* 2015;236:45–53 [CrossRef Medline](#)
4. Fujimura M, Shimizu H, Mugikura S, et al. **Delayed intracerebral hemorrhage after superficial temporal artery-middle cerebral artery anastomosis in a patient with moyamoya disease: possible involvement of cerebral hyperperfusion and increased vascular permeability.** *Surg Neurol* 2009;71:223–27 [CrossRef Medline](#)
5. Fushimi Y, Okada T, Takagi Y, et al. **Voxel based analysis of surgical revascularization for moyamoya disease: pre- and postoperative SPECT studies.** *PLoS One* 2016;11:e0148925 [CrossRef Medline](#)
6. Guzman R, Lee M, Achrol A, et al. **Clinical outcome after 450 revascularization procedures for moyamoya disease.** *J Neurosurg* 2009;111:927–35 [CrossRef Medline](#)
7. Miyoshi K, Chida K, Kobayashi M, et al. **Two-year clinical, cerebral hemodynamic and cognitive outcomes of adult patients undergoing medication alone for symptomatically ischemic moyamoya disease without cerebral misery perfusion: a prospective cohort study.** *Neurosurgery* 2018;84:1233–41 [CrossRef Medline](#)
8. Nam KW, Cho WS, Kwon HM, et al. **Ivy sign predicts ischemic stroke recurrence in adult moyamoya patients without revascularization surgery.** *Cerebrovasc Dis* 2019;47:223–30 [CrossRef Medline](#)
9. Williams DS, Detre JA, Leigh JS, et al. **Magnetic resonance imaging of perfusion using spin inversion of arterial water.** *Proc Natl Acad Sci USA* 1992;89:212–16 [CrossRef Medline](#)
10. Alsop DC, Detre JA. **Reduced transit-time sensitivity in noninvasive magnetic resonance imaging of human cerebral blood flow.** *J Cereb Blood Flow Metab* 1996;16:1236–49 [CrossRef Medline](#)
11. Detre JA, Samuels OB, Alsop DC, et al. **Noninvasive magnetic resonance imaging evaluation of cerebral blood flow with acetazolamide challenge in patients with cerebrovascular stenosis.** *J Magn Reson Imaging* 1999;10:870–75 [CrossRef Medline](#)
12. Goetti R, Warnock G, Kuhn FP, et al. **Quantitative cerebral perfusion imaging in children and young adults with moyamoya disease: comparison of arterial spin-labeling-MRI and H(2)[(15)O]-PET.** *AJNR Am J Neuroradiol* 2014;35:1022–28 [CrossRef Medline](#)
13. Yun TJ, Sohn CH, Han MH, et al. **Effect of delayed transit time on arterial spin labeling: correlation with dynamic susceptibility contrast perfusion magnetic resonance in moyamoya disease.** *Invest Radiol* 2013;48:795–802 [CrossRef Medline](#)
14. Noguchi T, Kawashima M, Irie H, et al. **Arterial spin-labeling MR imaging in moyamoya disease compared with SPECT imaging.** *Eur J Radiol* 2011;80:e557–62 [CrossRef Medline](#)
15. Hara S, Tanaka Y, Ueda Y, et al. **Noninvasive evaluation of CBF and perfusion delay of moyamoya disease using arterial spin-labeling MRI with multiple postlabeling delays: comparison with 15O-gas PET and DSC-MRI.** *AJNR Am J Neuroradiol* 2017;38:696–702 [CrossRef Medline](#)
16. Gunther M. **Highly efficient accelerated acquisition of perfusion inflow series by cycled arterial spin labeling.** In: *Proceedings of the 15th Annual Meeting of International Society of Magnetic Resonance in Medicine and the European Society for Magnetic Resonance in Medicine and Biology*, Berlin, Germany; May 19–25, 2007
17. Wells JA, Lythgoe MF, Gadian DG, et al. **In vivo Hadamard-encoded continuous arterial spin-labeling (H-CASL).** *Magn Reson Med* 2010;63:1111–18 [CrossRef Medline](#)

18. Fan AP, Khalighi MM, Guo J, et al. **Identifying hypoperfusion in moyamoya disease with arterial spin labeling and an [15O]-water positron emission tomography/magnetic resonance imaging normative database.** *Stroke* 2019;50:373–80 [CrossRef Medline](#)
19. Wang R, Yu S, Alger JR, et al. **Multi-delay arterial spin-labeling perfusion MRI in moyamoya disease: comparison with CT perfusion imaging.** *Eur Radiol* 2014;24:1135–44 [CrossRef Medline](#)
20. Guo J, Holdsworth SJ, Fan AP, et al. **Comparing accuracy and reproducibility of sequential and Hadamard-encoded multidelayer pseudocontinuous arterial spin-labeling for measuring cerebral blood flow and arterial transit time in healthy subjects: a simulation and in vivo study.** *J Magn Reson Imaging* 2018;47:1119–32 [CrossRef Medline](#)
21. Chang LT. **A method for attenuation correction in radionuclide computed tomography.** *IEEE Trans Nucl Sci* 1978;25:638–43 [CrossRef](#)
22. Setta K, Kojima D, Shimada Y, et al. **Accuracy of brain perfusion single-photon emission computed tomography for detecting misery perfusion in adult patients with symptomatic ischemic moyamoya disease.** *Ann Nucl Med* 2018;32:611–19 [CrossRef Medline](#)
23. Nishimiya M, Matsuda H, Imabayashi E, et al. **Comparison of SPM and NEUROSTAT in voxelwise statistical analysis of brain SPECT and MRI at the early stage of Alzheimer's disease.** *Ann Nucl Med* 2008;22:921–27 [CrossRef Medline](#)
24. Takeuchi R, Matsuda H, Yoshioka K, et al. **Cerebral blood flow SPET in transient global amnesia with automated ROI analysis by 3DSRT.** *Eur J Nucl Med Mol Imaging* 2004;31:578–89 [CrossRef Medline](#)
25. Soonawala D, Amin T, Ebmeier KP, et al. **Statistical parametric mapping of (99m)Tc-HMPAO-SPECT images for the diagnosis of Alzheimer's disease: normalizing to cerebellar tracer uptake.** *Neuroimage* 2002;17:1193–1202 [CrossRef Medline](#)
26. Ohnishi T, Yano T, Nakano S, et al. **Acetazolamide challenge and technetium-99m-ECD versus iodine-123-IMP SPECT in chronic occlusive cerebrovascular disease.** *J Nuc Med* 1997;38:1463–67 [Medline](#)
27. Alsop DC, Detre JA, Golay X, et al. **Recommended implementation of arterial spin-labeled perfusion MRI for clinical applications: a consensus of the ISMRM Perfusion Study Group and the European Consortium for ASL in dementia.** *Magn Reson Med* 2015;73:102–16 [CrossRef Medline](#)